

1 **Characterisation of *Staphylococcus aureus* lipids by**
2 **nanoelectrospray ionisation tandem mass**
3 **spectrometry (nESI-MS/MS)**

4
5 Simon A. Young^{1*}, Andrew P. Desbois², Peter J. Coote¹ and Terry K.
6 Smith¹

7 ¹School of Biology, Biomedical Sciences Research Complex, University of St Andrews, The
8 North Haugh, St Andrews, Fife, KY16 9ST, UK;

9 ²Institute of Aquaculture, Faculty of Natural Sciences, University of Stirling, Stirlingshire, FK9
10 4LA

11

12

13 *Corresponding author

14 E-mail: say2@st-andrews.ac.uk (SY)

15

16

17

18 **Abstract**

19 *Staphylococcus aureus* is a major opportunistic pathogen that is exposed to antimicrobial
20 innate immune effectors and antibiotics that can disrupt its cell membrane. An
21 understanding of *S. aureus* lipid composition and its role in defending the cell against
22 membrane-disrupting agents is of fundamental importance. Common methods for
23 characterising lipid profiles suffer shortcomings such as low sensitivity of detection and
24 inferior resolution of the positional assignments of fatty acid chains in lipids. This present
25 study developed a rapid and sensitive nano-electrospray ionisation tandem mass
26 spectrometry (nESI-MS/MS) method to characterise the lipid composition of three
27 commonly studied *S. aureus* isolates: Newman, Mu50 and BB270. Confirming previous
28 studies, nESI-MS/MS revealed that phosphatidylglycerols were most abundant in *S. aureus*
29 membranes, while diglucosyldiacylglycerols and lysyl-phosphatidylglycerols were also
30 detected. Positional assignments for individual fatty acid chains within these lipids were also
31 determined. Concomitantly, gas chromatography mass spectrometry of the fatty acids
32 validated the molecular characterization and showed the principal species present in each
33 strain were predominately anteiso- and iso-branched chain fatty acids. Though the fatty acid
34 and lipid profiles were similar between the *S. aureus* strains, this method was sufficiently
35 sensitive to distinguish minor differences in lipid composition. In conclusion, this nESI-
36 MS/MS methodology can characterise the role of lipids in antimicrobial resistance, and may
37 even be applied to the rapid diagnosis of drug-resistant strains in the clinic.

38

39 Introduction

40 As a Gram-positive bacterium found in the respiratory tract and on the skin of
41 healthy humans, *Staphylococcus aureus* is a major opportunistic pathogen responsible for a
42 range of community-acquired and nosocomial topical or systemic infections [1]. These
43 infections are treated with various classes of antibiotics, including agents that exert their
44 antimicrobial action by disrupting the bacterial cell membrane, such as daptomycin [2].
45 Moreover, many innate immunity defence effectors that act during the early stages of
46 infection, such as free fatty acids and cationic antimicrobial peptides (AMPs), also exert
47 antimicrobial action through targeting the integrity and functioning of the cell membrane
48 [3,4,5].

49 The major components of cell membranes are phospholipids, which form a
50 semipermeable barrier to maintain cell homeostasis and prevent the entry of harmful
51 substances. Phospholipid-containing membranes can permit bacteria to persist in the face
52 of external hazards such as osmotic stress or extremes of pH, and they play an integral role
53 in infection, acting as a barrier to antibiotics and host defense mechanisms [6]. Far from
54 being static structures, bacteria constantly modify the lipid composition of their membranes
55 in response to changes in the physiological environment, such as temperature, osmolarity,
56 salinity and pH [7]. Thus, it is of fundamental and clinical importance to gain a detailed
57 understanding of the composition of the *S. aureus* membrane and the role that changes in
58 lipid composition might render the cells less or more susceptible to the action of
59 membrane-disrupting antimicrobial agents.

60 The membranes of *S. aureus* have a preponderance of three phospholipids,
61 phosphatidylglycerol (PG), lysyl-phosphatidylglycerol (L-PG) and cardiolipin (CL), in addition
62 to other non-polar, glycosylated or conjugated lipid species [8]. Various approaches have
63 been used to characterise this lipid composition; most studies have utilised column
64 chromatography and two-dimensional thin-layer chromatography (2D-TLC) to provide basic
65 identification and chemical composition of lipid species [9,10]. Initially such characterisation
66 was performed on protoplasts derived from late-logarithmic or stationary phase *S. aureus*
67 cultures, thereby providing only a restricted view of the lipid composition. Long-term
68 radiolabelling of logarithmically growing bacteria with either [¹⁴C]acetate or [2-³H]glycerol
69 helped to provide a more complete picture of the lipid content when analysed by 2D-TLC
70 [11]. This provided an estimate for the relative abundances of the different lipid species in
71 the cell membranes, notably ~50% PG, ~20% diacylglycerol, ~10% L-PG, ~7%
72 diglucoxydiacylglycerol, ~1% CL, ~1% monoglucoxydiacylglycerol and ~5% of the cell wall
73 polymer lipoteichoic acid (LTA) [11]. Interestingly, CL content has been found to increase in
74 stationary phase [12] and under conditions of high salt [13]. When transitioning from
75 exponential growth to stationary phase CL content increases six-fold and this is
76 accompanied by a corresponding reduction in PG content, though the relative abundance of
77 L-PG remains constant [12]. Nevertheless, while 2D-TLC can provide accurate quantification
78 of each lipid class, it requires large amounts of lipid extracts and does not provide specificity
79 with regard to individual molecular species [14]. The application of targeted mass
80 spectrometry methods has provided some insight into the chemical composition of specific
81 *S. aureus* lipids [15,16], while gas chromatography mass spectrometry (GC-MS) has proved
82 successful in determining the specific fatty acid composition of *S. aureus* following diverse
83 genetic, chemical and environmental manipulations [17,18,19].

84 Nevertheless, a need exists for a rapid, sensitive and accurate quantitative method
85 to characterise in detail the lipid composition of the *S. aureus* cell membrane. The recent
86 applications of two distinct liquid chromatographic (LC) MS approaches, reversed-phase LC-
87 MS [20] and hydrophilic interaction LC-ion mobility-MS [21], have addressed some of the
88 limitations in earlier methodologies. Both of these studies describe similar, but not identical
89 *S. aureus* lipidomes, but these remain incomplete, as the authors did not obtain positional
90 assignments for the individual fatty acid chains to enable a full characterisation of each lipid
91 species. While it is common to use high-performance liquid chromatography (HPLC)
92 methodologies to separate lipids prior to MS detection, this is not essential because of the
93 relatively simple nature and lack of diversity of the *S. aureus* lipidome. In addition, LC-MS
94 approaches are time consuming and require significant downstream data processing and
95 analysis. To this end, we have utilised nanoelectrospray mass spectrometry (nESI-MS and
96 nESI-MS/MS) in combination with a direct infusion non-targeted (shotgun) methodology to
97 perform detailed characterisation of the lipid profile and fatty acid composition of the
98 abundant lipids in *S. aureus* cell membranes. This approach (in addition to subsequent GC-
99 MS analysis of fatty acid chains) provides a rapid and convenient way to sensitively compare
100 membrane lipid compositions between *S. aureus* strains.

101

102

103 **Materials and methods**

104 ***S. aureus* culture and lipid extraction**

105 All reagents and culture media were purchased from Sigma-Aldrich Ltd. *S. aureus* Newman
106 (methicillin-susceptible; MSSA), BB270 (methicillin-resistant; MRSA) and Mu50 (MRSA and
107 vancomycin intermediate-resistant) were sourced and cultured in Müller-Hinton broth as
108 described previously [22]. Briefly, each bacterial strain was prepared by inoculation of a
109 colony from an agar plate into 10 ml Müller-Hinton broth and cultured at 37°C with shaking
110 until reaching an $OD_{600nm} = 1$ ($\sim 1 \times 10^9$ colony-forming units [cfu]). Bacterial cells were
111 harvested ($1000 \times g$, 10 min), washed in PBS before a repeat centrifugation and removal of
112 the supernatant. Lipids were extracted according to the Bligh-Dyer method [23], dried under
113 nitrogen, and stored at 4°C until analysis by mass spectrometry.

114

115 **Fatty acid methyl ester preparation and GC-MS analysis**

116 The global fatty acid composition of the *S. aureus* strains was characterised and quantified
117 by their conversion to fatty acid methyl esters (FAME) followed by GC-MS analysis. Briefly,
118 duplicate aliquots of the lipid extracts equivalent to 1×10^8 cfu were transferred to 2-ml
119 glass vessels and dried under nitrogen gas. Fatty acids were released from intact lipids by
120 base hydrolysis using 500 μ l of concentrated ammonia and 500 μ l of 50% propan-1-ol (in
121 water), followed by incubation for 5 h at 50°C. After cooling to room temperature the
122 samples were evaporated to dryness with nitrogen gas and then dried twice more after
123 washing in 200 μ l of methanol:water (1:1) to remove all traces of ammonia. The protonated
124 fatty acids were then extracted by partitioning between 500 μ l of 20 mM HCl and 500 μ l of

125 ether, before the aqueous phase was re-extracted with fresh ether (500 μ l) and the
126 combined ether phases were dried under nitrogen gas in a glass tube. The fatty acids were
127 converted to methyl esters by adding diazomethane ($3 \times 20 \mu$ l aliquots) to the dried residue,
128 while on ice. After 30 min the samples were allowed to warm to room temperature and left
129 to evaporate to dryness in a fume hood. The dried FAME samples were dissolved in 20 μ l
130 dichloromethane and analysed by injection of 1 μ l into a GC-MS (GC-6890N, MS detector-
131 5973; Agilent Technologies) using a ZB-5 column (30 m \times 25 mm \times 25 mm; Phenomenex)
132 operating a temperature program of 50°C for 10 min, followed by a rising gradient to 220°C
133 at 5°C min⁻¹, and held at 220°C for a further 15 min. Mass spectra were continuously
134 acquired in the range of 50–500 atomic mass units (amu) and peak identification was
135 performed by comparison of retention times and fragmentation patterns with a standard
136 bacterial FAME mixture containing both odd and even fatty acid chains (Supelco 47080-U;
137 Sigma-Aldrich Ltd).

138

139 **nESI-MS/MS analysis**

140 Lipid extracts were analysed by nESI-MS and nESI-MS/MS following the method of Lilley *et*
141 *al.* [24]. Briefly, total lipid extracts were dissolved in 100 μ l of chloroform:methanol (1:2)
142 and analysed with a triple quadrupole time of flight (QTOF) mass spectrometer equipped
143 with a nanoelectrospray source (4000 QTrap; AB SCIEX). Each sample (15 μ l) was delivered
144 using a Nanomate interface (Advion, Inc.) in direct infusion mode (~ 125 nl min⁻¹). The lipid
145 extracts were analysed in both positive and negative ion modes using a capillary voltage of
146 1.25 kV. MS/MS scanning (precursor, daughter and neutral loss) were performed using
147 nitrogen as the collision gas and each spectrum encompassed at least 50 repetitive scans.

148 Tandem mass spectra were obtained with collision energies as follows: 20-35 V, neutral loss
149 scanning of m/z 300 in positive ion mode to detect L-PG; 50 V, selected precursor ion (m/z
150 211, 225, 239, 253, 267, 281, 295, 309, 323) scanning in negative mode. MS/MS
151 fragmentation/daughter ion scanning was performed in positive and negative modes with
152 collision energies between 35–100 V. For each sample, data were acquired in two distinct
153 scan windows (600–1000 m/z and 1000–1500 m/z) in both positive and negative modes.
154 The assignment of individual lipid species was based upon a combination of survey,
155 daughter and precursor scans, as well as submitting parent ion masses to the LIPID MAPS
156 database at the Nature Lipidomics Gateway (<http://www.lipidmaps.org>).

157

158 Results and discussion

159 Fatty acid composition

160 GC-MS analysis of the FAME prepared from total lipid extracts from the three
161 laboratory-cultured *S. aureus* strains, BB270, Newman and Mu50, revealed that the
162 principal fatty acid species ranged from C14 to C20 in length (Fig 1A). In addition, the
163 analysis confirmed the dominant presence of iso- and anteiso-branched chain fatty acids,
164 common to Gram-positive bacteria [25]. All three strains showed similar profiles, although
165 when cultured in Müller-Hinton broth the BB270 lab strain consistently had a reduced
166 percentage (4.53 ± 0.25 %) of longer straight- and branched-chain fatty acids (specifically i-
167 19:0, a-19:0, 19:0, 20:0) relative to the Newman (7.72 ± 0.47 %) and Mu50 (10.56 ± 0.27 %)
168 strains. Grouping the fatty acids by structure as straight, anteiso- and iso-branched,
169 confirmed that the strains have relatively similar proportions of each type of fatty acid (Fig
170 1B). However, calculating the specific ratios of branched- to straight-chain fatty acids
171 revealed values of 4.57 ± 0.20 (BB270), 10.9 ± 0.36 (Newman) and 9.06 ± 0.23 (Mu50),
172 indicating the BB270 strain to have a greater proportion of saturated straight-chain fatty
173 acids. Notably this was due to a reduced proportion of anteiso-branched chain fatty acids, as
174 the proportion of iso-branched chains remained similar between the strains (Fig 1B).
175 Overall, the fatty acid composition of these strains closely matched those of other *S. aureus*
176 strains cultured in Müller-Hinton broth [26].

177 **Fig 1. Fatty acid analysis from three different *S. aureus* strains.** A) Total fatty acid
178 composition of lipids from three *S. aureus* strains: BB270 (black), Newman (dark grey) and
179 Mu50 (light grey). B) Relative percentage composition of straight, anteiso-branched and iso-
180 branched chain fatty acids of lipids from three *S. aureus* strains: BB270 (black), Newman

181 (dark grey) and Mu50 (light grey). C) Biosynthesis, including the FASII cycle, of the straight-
182 and branched-chain fatty acids in *S. aureus*, illustrating the functional differences between
183 the pathways. See S1 Table for a description of the genes involved in the pathways and their
184 functions. Circled molecules show the origin for the structural differences between the
185 different fatty acid types.

186

187 A simplified biosynthetic pathway of the straight- and branched-chain fatty acids
188 identified by GC-MS in *S. aureus* is shown in Fig 1C. The specific genes that utilise the various
189 molecular precursors to produce the straight-, branched-anteiso, branched-iso (odd chain)
190 and branched-iso (even chain) fatty acids of these three *S. aureus* strains are listed in S1
191 Table, alongside other representative Gram-positive bacteria. As with most bacteria,
192 straight-chain fatty acids are formed via pyruvate through the synthesis of malonyl-CoA that
193 enters the normal type II fatty acid synthesis (FASII) pathway. The branched-chain fatty acids
194 have amino acid precursors (valine, leucine and isoleucine) that, unlike pyruvate, are
195 processed by an alternative suite of enzymes and enter the FASII pathway as specific
196 branched-chain acyl-CoA substrates. Fig 1C highlights that it is the amino acid side chains
197 that give the branched-chain fatty acids their ultimate structural identity.

198

199 **Lipid composition**

200 **Phosphatidylglycerols**

201 Survey scans (nESI-MS) in negative ion mode of lipids extracted from each *S. aureus*
202 strain revealed the profile of the most abundant lipid to be PG, with [M-H]⁻ ions ranging
203 between m/z 679 – 777 (Fig 2). Submission of the parent masses to the LIPID MAPS

204 database determined the PG lipids had a total fatty acid chain content of 29–36 carbons.
205 This lipid profile was highly similar between each strain with only minor differences
206 observed; the relative abundance of the greater molecular weight lipids (m/z 735 and
207 higher) was lowest in BB270 (Fig 2A), greater in Newman (Fig 2B) and greatest in Mu50 (Fig
208 2C), and there were corresponding reductions in the PG species containing shorter fatty acid
209 chains.

210 **Fig 2. Survey scans in negative mode (640–800 m/z).** Phosphatidylglycerol species of three
211 *S. aureus* strains: A) BB270 B) Newman and C) Mu50.

212

213 In ESI-MS/MS, the established rule is that the more abundant daughter ions are
214 those that result from loss of the acyl chain (as a neutral loss or as the ketene) from the 2
215 position (*sn*-2) of the glycerol backbone of the phospholipid [27]. Thus, parent ion
216 fragmentation by nESI-MS/MS determined the specific composition and position of the acyl
217 chains for each PG molecule (as an example, see the fragmentation spectrum of PG C32:0 in
218 S1A Fig). The fatty acid composition of the principal isomers for each parent ion from the
219 BB270 strain are noted in Fig. 2, while S2 Table also details the composition of the less
220 abundant isomers. This revealed that it was always the shorter acyl chain of the two
221 substituents that was found at the *sn*-2 position, most frequently a C15:0 fatty acid, with
222 other saturated fatty acids in some of the minor PG species. This classification by nESI-
223 MS/MS mirrored the total fatty acid abundance obtained by GC-MS, where C15:0 and C17:0
224 fatty acids predominated in the profiles (Fig 1A). As such, it is expected that the *sn*-1-linked
225 C17:0 and *sn*-2-linked C15:0 fatty acids of the abundant PG molecule (m/z 721.4, C32:0) will

226 predominantly be the anteiso-C17:0 and anteiso-C15:0 branched-chain versions identified
227 to be the most abundant by GC-MS.

228

229 **Diglucosyldiacylglycerols**

230 ESI-MS survey scans in positive ion mode of lipids extracted from the three *S. aureus*
231 strains revealed the presence of an abundant neutral lipid, diglucosyl-diacylglycerol (Glc₂-
232 DAG), with various [M+Na]⁺ ions ranging between 859–971 m/z (Fig 3). Glc₂-DAG is the
233 glycolipid that provides the membrane anchor for the principal cell wall polymer LTA [28].
234 Daughter ion fragmentation in positive mode confirmed each lipid was detected as a sodium
235 adduct [M+Na]⁺ and total fatty acid chains ranged between 28–36 carbons (as an example,
236 see the fragmentation spectrum in S2 Fig). Although all three strains had similar Glc₂-DAG
237 profiles with the dominant molecule again being C32:0, it is notable that, unlike BB270,
238 Newman and Mu50 have Glc₂-DAG lipids with fatty acid contents between 30–36 carbons
239 with no shorter chain C28:0 or C29:0 detected. As Glc₂-DAG lipids can be detected in
240 negative mode as well as positive mode, positional assignments of the fatty acid chains
241 were deduced from daughter ion spectra acquired from fragmentation of the lipids in both
242 modes. It is important to note that in the fragmentation of molecular species in positive
243 mode for glycolipids such as these, the more abundant daughter ions detected are those
244 resulting from the loss of the acyl chain at the *sn*-1 rather than *sn*-2 position [29].

245 **Fig 3. Survey scans in positive mode (830–980 m/z).** Diglucosyl-diacylglycerol species of
246 three *S. aureus* strains: A) BB270 B) Newman and C) Mu50.

247

248 **Lysyl-phosphatidylglycerols**

249 Neutral loss scans of 300 Da in positive ion mode of the three *S. aureus* lipid extracts
250 revealed the profile of lysyl-PG, with peaks ranging 809–893 m/z (Fig 4). Daughter ion
251 fragmentation in positive mode indicated each molecular species had a total fatty acid chain
252 content ranging between 29-35 carbons (as an example, see fragmentation spectrum in S3
253 Fig) and showed that all three strains contained the same lipids, with only minor differences
254 in their proportions. Like the PG that acts as the substrate for the formation of lysyl-PG, the
255 C32:0 species is the dominant lipid in the profile, but a longer chain C36:0-containing lysyl-
256 PG was not detected in any of the strains. Like Glc₂-DAG, lysyl-PG can be detected in
257 negative ion mode as well as positive and so the specific composition of each molecular
258 species was established by daughter ion fragmentation in both modes. Again the acyl chain
259 distribution was comparable to the composition of the other lipids (S2 Table) and mirrored
260 the total fatty acid abundance obtained by GC-MS.

261 **Fig 4. Neutral loss (300 Da) scans in positive mode (800–920 m/z).** Lysyl-
262 phosphatidylglycerol species of three *S. aureus* strains: A) BB270 B) Newman and C) Mu50.

263

264 **Cardiolipins**

265 The identification and characterisation of CL species in *S. aureus* can be difficult,
266 mainly due to the minor abundance (~1%) present in exponential growth phase bacteria
267 such as used in this present study [12]. Consequently, using the standard Bligh-Dyer
268 extraction method resulted in limited detection of CL, and only in the BB270 and Newman
269 strains (S4 Fig). The apparent lack of CL in the Mu50 strain might be due to the low
270 efficiency of cardiolipin extraction from the cell membranes due to the thicker cell walls of
271 the Mu50 strain [30]. In negative mode ESI-MS, the BB270 and Newman strains typically

272 showed CL as $[M-2H+Na]^-$ ions, though minor $[M-H]^-$ species were also detected, a common
273 observation when using this type of nESI-QTOF mass spectrometer [31]. Submission of the
274 parent masses to the LIPIDMAPS database established that each molecular species had a
275 total fatty acid chain content ranging 59–69 carbons and parent ion fragmentation by ESI-
276 MS/MS determined the composition of the acyl chains (S2 Table). Predominantly, the fatty
277 acid composition reflected the abundance of the PG species available from which to
278 synthesise CL, though there is an absence of C19:0 and C20:0 due to the lack of detection of
279 any higher molecular weight (i.e. greater than C69:0) species. Due to the difficulties in
280 extraction and analysis, CL studies of *S. aureus* would benefit from targeted lipid analysis, a
281 focus on stationary phase bacteria, and use of a modified Bligh-Dyer lipid extraction
282 protocol utilising a pre-treatment step with lysostaphin [32], which is recommended for *S.*
283 *aureus* strains with unusually thick cell walls [30].

284

285 **Unsaturated lipids**

286 Observable in some of the lipid profiles were a series of minor peaks that were 2
287 amu less than the equivalent major ions, suggesting the existence of lipids with unsaturation
288 (specifically a single double bond) in some of the fatty acid chains. These ions are more
289 prevalent in the PG survey scans and particularly prominent in the BB270 profile (Fig 2A).
290 Fragmentation of these parent masses confirmed that a single fatty acid chain was
291 unsaturated in each PG molecule (S2 table). Fragmentation also revealed that the double
292 bond could be present in either an odd or even chain fatty acid in either the *sn*-1 or *sn*-2
293 position with no apparent specificity (S1B Fig). Though highly sensitive and analytical, nESI-
294 MS/MS is unable to define the specific location of a double bond within the fatty acid chain.
295 Single unsaturated fatty acids were detected also in some lysyl-PG and again were more

296 prevalent in the BB270 strain, with fewer observed in the Newman strain and a complete
297 absence in Mu50 (Fig 4). The fatty acid compositions of the unsaturated lysyl-PG species
298 from BB270 were found to be very similar to the equivalent unsaturated PG species (S2
299 Table). Remarkably for all three strains, no unsaturation was detected in the Glc₂-DAG lipids
300 (Fig 3). As an alternative method to identify the presence of unsaturated fatty acids,
301 precursor ion scanning was employed to detect parent PG species ions that contained
302 fragments corresponding to unsaturated fatty acids (S5 Fig). For example, searching for a
303 fragment ion of m/z 225 (C14:1) revealed no parent ions (this is in agreement with C14:1 not
304 being detected in PG), while searching for parents of m/z 239 (C15:1) showed ions at m/z
305 691, 705, 719, 733, 747 and 761, in agreement with the daughter ion fragmentation of these
306 parent ion species (S5A Fig). Conversely, m/z 267 (C17:1) was identified principally in a
307 parent ion at m/z 719, the dominant molecular species indicated by fragmentation to
308 contain the C17:1 fatty acid (S5B Fig). Furthermore, parent ion scanning revealed the
309 existence of a small proportion of a doubly unsaturated (17:1/15:1) PG (m/z 717, S5 Fig and
310 S2 Table).

311 The presence of unsaturated lipids in *S. aureus* is somewhat controversial, with a
312 common assumption in the community that the biophysical role of unsaturated fatty acids is
313 substituted by the abundant branched-chain fatty acids in Gram-positive bacteria [25].
314 Indeed, in two recent LC-MS studies on *S. aureus* lipids, one reported only saturated lipids to
315 exist in Col and Newman strains [20], while the other on the N315 strain detected lipids
316 containing unsaturated fatty acid chains (specifically C29:1 to C35:1 PG species) [21], though
317 no comment was made on the existence of these molecular species. However, it is common
318 to have minor variations in fatty acid contents and thus the profiles of bacterial lipidomes
319 due to variations in growth phase, choice of strain and culture media, and indeed these

320 earlier studies utilised brain-heart infusion media [20,21]. As the approved medium used for
321 antimicrobial susceptibility testing, Müller-Hinton broth was selected for this present study
322 to allow for future studies of the phenotyping of lipid and membrane changes induced by
323 antimicrobial compounds.

324 To assess whether the detection of unsaturated fatty acids was specific to culture of
325 *S. aureus* in Müller-Hinton broth, we analyzed the lipids of each of the three strains after
326 culture in tryptic soy broth (TSB) and identified similar levels of unsaturated lipids from
327 bacteria harvested under both culture conditions. S6 Fig shows the alternative profile of PG
328 lipids from the Newman strain cultured in TSB (S6A Fig) in comparison to MH (S6B Fig).
329 Fragmentation illustrated that the fatty acid composition of the PG species varied noticeably
330 from that observed after culture in Müller-Hinton broth, with an increase in even-chain
331 saturated FA relative to the branched-chain FA (S6 Fig). This observation concurs with a
332 recent study that examined the fatty acid profiles of *S. aureus* after culture in diverse media
333 including Müller-Hinton broth and TSB [26]. Unfortunately, GC-MS analysis of FAME from
334 the three *S. aureus* strains failed to detect unsaturated fatty acids (Fig 1A). However, as the
335 longer saturated-chain C21:0 fatty acid, observed in fragmentation of both PG and Glc₂-
336 DAG, was also absent from the FAME data, the lack of detection by the GC-MS is
337 conceivably a question of sensitivity. While no obvious genes for the biosynthesis of
338 unsaturated FA have been identified in the genomes of BB270, Newman and Mu50, a recent
339 study showed that different strains of *S. aureus* cultured in bovine serum can readily acquire
340 FA from the medium and incorporate these into their lipids such that monounsaturated FA
341 can compose up to 30% of the total FA content [26]. Importantly, this shows that in a more
342 physiologically relevant setting, *S. aureus* is flexible regarding the degree of fatty acid
343 unsaturation present in lipids in its membranes.

344 Uptake and incorporation of exogenous fatty acids into *S. aureus* lipids (independent
345 of *de novo* synthesis by FASII) is a recent discovery and occurs by a fatty acid kinase-
346 dependent pathway [33]. Protonated fatty acids diffuse into the cell where they are bound
347 by two fatty-acid binding proteins (FakB1/FakB2), with saturated fatty acids binding to
348 FakB1 and unsaturated fatty acids to FAKB2 [34]. Using ATP FakA phosphorylates the fatty
349 acid to acyl-phosphate (acyl-PO₄), which can then be used as a substrate by the membrane-
350 bound acyltransferase PlsY. *FakA* deletion prevents the incorporation of exogenous fatty
351 acids into lipids and can lead to a stress response, increased resistance to antimicrobial
352 peptides and decreased production of virulence factors [35]. Furthermore, when cultured in
353 the presence of porcine liver extracts *S. aureus* bacteria with non-synonymous mutations in
354 the malonyl CoA-acyl carrier protein transacylase (*fabD*) gene bypass the FASII pathway and
355 incorporate long-chain polyunsaturated fatty acids such as C20:4 into their membranes [36].
356 Examination of a large panel of clinical isolates has indicated that it could be a common
357 strategy of *S. aureus* to incorporate exogenous FA, overcoming its reliance on endogenous
358 FA biosynthesis, and thus rendering ineffective FASII inhibitors such as the widely used
359 biocide triclosan [37].

360

361 **Biosynthesis of phospholipids**

362 All the *S. aureus* lipids characterised in this present study are synthesised by an
363 interlinked biosynthetic pathway (Fig 5), and the respective genes that function in this
364 pathway are presented for the three *S. aureus* strains analysed herein, and homologous
365 genes from other Gram-positive bacteria, in S3 Table. Kuhn and colleagues describe in more
366 detail the regulation of lipid biosynthesis in *S. aureus* [38].

367 **Figure 5: Lipid biosynthesis in *S. aureus*.** Depicting the metabolites and proteins involved in
368 the discrete pathways. The precursor molecules for lipid biosynthesis are underlined. Boxed
369 molecules are those lipids that are readily detected in *S. aureus* cell membranes. A dotted
370 line illustrates a theoretical recycling route from phosphatidic acid (PA) to diacylglycerol
371 (DAG) yet to be confirmed experimentally. See S3 Table for a description of the genes
372 involved in the pathways and their functions.

373

374 Briefly, synthesis of phospholipids in *S. aureus* is initiated by acylation of glycerol-3-
375 phosphate (Gro-3-P) with fatty acids generated by the FASII pathway. Initially, the acyl-
376 carrier protein substrates (acyl-ACP) produced by the FASII pathway are converted to acyl-
377 PO₄ [39] by the essential enzyme PlsX, whose deletion creates fatty acid auxotrophic *S.*
378 *aureus* [33]. Subsequently, the similarly essential membrane-bound Gro-3-P acyltransferase
379 PlsY uses the acyl-PO₄ as substrate to form 1-acyl-Gro-3-P [40]. The second fatty acid is
380 transferred to the *sn*-2 position of acyl-Gro-3-P from acyl-ACP by the membrane-bound PlsC,
381 producing phosphatidic acid (PA).

382 Phospholipid synthesis continues with the production of cytidine diphosphate-
383 diacylglycerol (CDP-DAG) by CdsA from PA using cytidine triphosphate. As a CDP-DAG-
384 glycerol-3-phosphate 3-phosphatidyltransferase, PgsA then removes cytidine
385 monophosphate and adds Gro-3-P to produce phosphatidylglycerolphosphate (PGP) [41].
386 Interestingly, mutations in *PgsA* have been identified in a daptomycin-non-susceptibility
387 phenotype [42]. Significantly, the phosphatidylglycerophosphatase (PgpP) that removes the
388 terminal phosphate to yield PG, the major phospholipid of *S. aureus*, remains to be
389 identified [13]. Some of the PG pool is apportioned for further lipid synthesis, while some

390 PG is synthesized to CL by the phospholipase D-like CL synthases Cls1 and Cls2, which fuse
391 two PG molecules and release glycerol [43]. Cls1 seems to be necessary for CL synthesis only
392 under conditions of acid stress, while Cls2 is the general bulk CL synthase utilized under
393 normal culture conditions [32,44]. A relatively unusual but highly significant biological
394 process is the aminoacylation of PG with L-lysine, forming lysyl-PG, by the multiple peptide
395 resistance factor protein MprF that also translocates the cationic phospholipid from the
396 inner to outer leaflet of the plasma membrane [45]. *MprF* is not essential, but deletion
397 strains show much greater susceptibility to the detrimental effects of cationic antimicrobial
398 peptides and antibiotics [46] and are attenuated in animal infection models [45].

399 Finally, as a constituent of the major cell wall component LTA [47], there is
400 enormous demand for the Gro-P headgroup of PG, which requires the PG pool to be
401 replenished up to three times per bacterial cell cycle [11, 48]. LTA is a polymeric
402 glycerophosphate chain ($n \approx 24$) that is anchored in the plasma membrane by Glc₂-DAG. As
403 shown in Figure 6, this glycolipid anchor is synthesized with two consecutive glycosylations
404 of DAG by the glucosyltransferase YpfP using UDP-glucose to form Glc₂-DAG. Deletion of
405 *YpfP* results in the absence of Glc₂-DAG and as a consequence LTA anchors instead to the
406 DAG precursor, resulting in drastically reduced viability when cultured under certain
407 conditions, such as in 0.05 M phosphate buffer (pH 7.2) containing 0.85% NaCl at 37°C [28].
408 It is presumed that, as a putative glycolipid permease, LtaA translocates the Glc₂-DAG to the
409 outer leaflet of the plasma membrane, where the membrane-bound LtaS transfers 20–40
410 glycerophosphate molecules from PG lipids to the elongating glycolipid anchor [49]. The
411 DAG generated from this transfer is recycled by the DAG kinase DgkB that phosphorylates it
412 to PA, which can be re-utilized for further PG synthesis [50]. Unsurprisingly, deletion of *LtaS*

413 produces a *S. aureus* cell lacking in LTA [49] and that is unable to grow unless compensatory
414 mutations are present to increase the pool of the secondary messenger c-di-AMP [51].

415

416 **Conclusions**

417 In conclusion, this present study reports the application of a rapid, non-targeted nESI-
418 MS/MS lipidomic method allowing characterisation of three representative *S. aureus* strains.
419 This technology gives a high sensitivity of detection and provides a more complete
420 description of lipid composition in comparison to previous studies, including the positional
421 assignments of fatty acids. This enhanced sensitivity has enabled the detection of
422 comparatively minor differences in the lipid profiles of the *S. aureus* strains under
423 investigation. As a result it can be routinely employed to compare *S. aureus* lipid profiles,
424 which may assist with determining the role of membrane lipids in the development of
425 resistance to membrane-active antimicrobial agents, and could be developed even further
426 to diagnose drug-resistant strains in the clinic.

427

428 **Acknowledgments**

429 We gratefully acknowledge Ms. Leigh-Ann Booth (University of St Andrews) for assisting in
430 the assignment of lipid compositions from fragmentation spectra.

431

432

433 References

- 434 1 Crossley KB, Jefferson KK, Archer GL, Fowler VG. *Staphylococci in Human Disease*,
435 2nd ed. Chichester: John Wiley and Sons Ltd; 2009.
- 436 2 Daptomycin. National Institute for Health and Care Excellence. 2018. British
437 National Formulary. Available from:
438 <https://bnf.nice.org.uk/drug/daptomycin.html> [accessed 10/08/18].
- 439 3 Brogden NK, Mehalick L, Fischer CL, Wertz PW, Brogden, KA. The emerging role
440 of peptides and lipids as antimicrobial epidermal barriers and modulators of local
441 inflammation. *Skin Pharmacol Physiol*. 2012; 25: 167–181. doi:
442 10.1159/000337927.
- 443 4 Porter E, Ma DC, Alvarez S, Faull KF. Antimicrobial lipids: Emerging effector
444 molecules of innate host defense. *World J Immunol*. 2015;5: 51–61. doi:
445 10.5411/wji.v5.i2.51
- 446 5 Le PNT, Desbois AP. Antibacterial effect of eicosapentaenoic acid against *Bacillus*
447 *cereus* and *Staphylococcus aureus*: Killing kinetics, selection for resistance, and
448 potential cellular target. *Marine Drugs*. 2017;15: 334. doi: 10.3390/md15110334.
- 449 6 Kraus D, Peschel A. *Staphylococcus aureus* evasion of innate antimicrobial
450 defense. *Future Microbiol*. 2008;3: 437-51. doi: 10.2217/17460913.3.4.437.
- 451 7 Zhang YM, Rock CO. Membrane lipid homeostasis in bacteria. *Nat Rev Microbiol*.
452 2008;6: 222-33. doi: 10.1038/nrmicro1839.
- 453 8 Ratledge C, Wilkinson SG. *Microbial lipids*. London: Academic Press; 1988.
- 454 9 White DC, Frerman FE. Extraction, Characterization, and Cellular Localization of
455 the Lipids of *Staphylococcus aureus*. *J Bacteriol*. 1967; 94: 1854–1867.

- 456 10 Ward JB, Perkins MR. The chemical composition of the membranes of
457 protoplasts and L-forms of *Staphylococcus aureus*. Biochem J. 1968;106: 391–
458 400.
- 459 11 Koch HU, Haas R, Fischer W. The role of lipoteichoic acid biosynthesis in
460 membrane lipid metabolism of growing *Staphylococcus aureus*. Eur J Biochem.
461 1984;138: 357-363. doi: 10.1111/j.1432-1033.1984.tb07923.x.
- 462 12 Short SA, White DC. Metabolism of phosphatidylglycerol,
463 lysylphosphatidylglycerol, and Cardiolipin of *Staphylococcus aureus*. J Bacteriol.
464 1971;108: 219-26.
- 465 13 Kanemasa Y, Yoshioka T, Hayashi H. Alteration of the phospholipid composition
466 of *Staphylococcus aureus* cultured in medium containing NaCl. Biochim Biophys
467 Acta. 1972;280: 444-450. doi: 10.1016/0005-2760(72)90251-2.
- 468 14 Mishra NN, Bayer AS. Correlation of Cell Membrane Lipid Profiles with
469 Daptomycin Resistance in Methicillin-Resistant *Staphylococcus aureus*.
470 Antimicrob Agents Chemother. 2013;57: 1082–1085. doi: 10.1128/AAC.02182-
471 12.
- 472 15 Peter-Katalinic J, Fischer W. α -d-Glucopyranosyl-, d-alanyl- and l-lysylcardiolipin
473 from gram-positive bacteria: analysis by fast atom bombardment mass
474 spectrometry. J Lipid Res. 1998;39: 2286-2292.
- 475 16 Rubio A, Moore J, Varoglu M, Conrad M, Chu M, Shaw W, et al. LC-MS/MS
476 characterization of phospholipid content in daptomycin-susceptible and -
477 resistant isolates of *Staphylococcus aureus* with mutations in *mprF*. Mol Membr
478 Biol. 2012;29: 1-8. doi: 10.3109/09687688.2011.640948.

- 479 17 Mirani ZA, Jamil N. Effect of vancomycin on the cytoplasmic membrane fatty acid
480 profile of vancomycin-resistant and -susceptible isolates of *Staphylococcus*
481 *aureus*. J Infect Chemother. 2013;19: 24-33. doi: 10.1007/s10156-012-0447-y.
- 482 18 Singh VK, Hattangady DS, Giotis ES, Singh AK, Chamberlain NR, Stuart MK, et al.
483 Insertional inactivation of branched-chain alpha-keto acid dehydrogenase in
484 *Staphylococcus aureus* leads to decreased branched-chain membrane fatty acid
485 content and increased susceptibility to certain stresses. Appl Environ Microbiol.
486 2008;74: 5882-90. doi: 10.1128/AEM.00882-08.
- 487 19 Wang LH, Wang MS, Zeng XA, Liu ZW. Temperature-mediated variations in
488 cellular membrane fatty acid composition of *Staphylococcus aureus* in resistance
489 to pulsed electric fields. Biochim Biophys Acta. 2016;1858: 1791-800. doi:
490 10.1016/j.bbamem.2016.05.003.
- 491 20 Hewelt-Belka W, Nakonieczna J, Belka M, Bączek T, Namieśnik J, Kot-Wasik A.
492 Comprehensive methodology for *Staphylococcus aureus* lipidomics by liquid
493 chromatography and quadrupole time-of-flight mass spectrometry. J Chromatogr
494 A. 2014;1362: 62-74. doi: 10.1016/j.chroma.2014.08.020.
- 495 21 Hines KM, Waalkes A, Penewit K, Holmes EA, Salipante SJ, Werth BJ, et al.
496 Characterization of the mechanisms of daptomycin resistance among Gram-
497 positive bacterial pathogens by multidimensional lipidomics. mSphere.
498 2017;2:e00492-17. doi: 10.1128/mSphere.00492-17.
- 499 22 Desbois AP, Gemmell CG, Coote PJ. In vivo efficacy of the antimicrobial peptide
500 ranalexin in combination with the endopeptidase lysostaphin against wound and
501 systemic methicillin resistant *Staphylococcus aureus* (MRSA) infections. Int J
502 Antimicrob Agents. 2010;35: 559. doi: 10.1016/j.ijantimicag.2010.01.016.

- 503 23 Bligh E, Dyer W. A rapid method of total lipid extraction and purification. Can J
504 Biochem Physiol. 1959;37: 911–7. doi: 10.1139/o59-099.
- 505 24 Lilley AC, Major L, Young S, Stark MJR, Smith TK. The essential roles of cytidine
506 diphosphate-diacylglycerol synthase in bloodstream form *Trypanosoma*
507 *brucei*. Mol Microbiol. 2014;92: 453–470. doi: 10.1111/mmi.12553.
- 508 25 Cho KY, Salton MRJ. Fatty acid composition of bacterial membrane and wall
509 lipids. Biochimica et Biophysica Acta. 1966;116: 73-79. doi: 10.1016/0005-
510 2760(66)90093-2.
- 511 26 Sen S, Sirobhusanam S, Johnson SR, Song Y, Tefft R, Gatto C, et al. Growth-
512 Environment Dependent Modulation of *Staphylococcus aureus* Branched-Chain
513 to Straight-Chain Fatty Acid Ratio and Incorporation of Unsaturated Fatty Acids.
514 PLoS ONE. 2016;11: e0165300. doi: 10.1371/journal.pone.0165300.
- 515 27 Murphy RC. Mass spectrometry of lipids. Handbook of Lipid Research Vol 7. New
516 York: Springer US; 1993.
- 517 28 Kiriukhin MY, Debabov DV, Shinabarger DL, Neuhaus FC. Biosynthesis of the
518 Glycolipid Anchor in Lipoteichoic Acid of *Staphylococcus aureus* RN4220: Role of
519 YpfP, the Diglucoxydiacylglycerol Synthase. J Bact. 2001;183: 3506–3514. doi:
520 10.1128/JB.183.11.3506-3514.2001.
- 521 29 Guella G, Frassanito R, Mancini I. A new solution for an old problem: the
522 regiochemical distribution of the acyl chains in galactolipids can be established
523 by electrospray ionization tandem mass spectrometry. Rapid Commun Mass
524 Spectrom. 2003;17: 1982–1994. doi: 10.1002/rcm.1142.
- 525 30 Cui L, Murakami H, Kuwahara-Arai K, Hanaki H, Hiramatsu K. Contribution of a
526 thickened cell wall and its glutamine nonamidated component to the vancomycin

- 527 resistance expressed by *Staphylococcus aureus* Mu50. Antimicrob Agents
528 Chemother. 2000;44: 2276-2285. doi: 10.1128/AAC.44.9.2276-2285.2000
- 529 31 Beckedorf AI, Schäffer C, Messner P, Peter-Katalinić J. Mapping and sequencing
530 of cardiolipins from *Geobacillus stearothermophilus* NRS 2004/3a by positive and
531 negative ion nanoESI-QTOF-MS and MS/MS. J Mass Spectrom. 2002;37: 1086-94.
532 doi: 10.1002/jms.369.
- 533 32 Tsai M, Ohniwa RL, Kato Y, Takeshita SL, Ohta T, Saito S, et al. *Staphylococcus*
534 *aureus* requires cardiolipin for survival under conditions of high salinity. BMC
535 Microbiol. 2011;11: 13. doi: 10.1186/1471-2180-11-13.
- 536 33 Parsons JB, Frank MW, Jackson P, Subramanian C, Rock CO. Incorporation of
537 Extracellular Fatty Acids by a Fatty Acid Kinase-Dependent Pathway in
538 *Staphylococcus aureus*. Mol Microbiol. 2014;92: 234–245. doi:
539 10.1111/mmi.12556.
- 540 34 Parsons JB, Broussard TC, Bose JL, Rosch JW, Jackson P, Subramanian C, et al.
541 Identification of a two-component fatty acid kinase responsible for host fatty
542 acid incorporation by *Staphylococcus aureus*. Proc Natl Acad Sci. 2014;111:
543 10532-10537. doi: 10.1073/pnas.1408797111.
- 544 35 Li M, Rigby K, Lai Y, Nair V, Peschel A, Schitteck B, et al. *Staphylococcus aureus*
545 mutant screen reveals interaction of the human antimicrobial peptide dermcidin
546 with membrane phospholipids. Antimicrob Agents Chemother. 2009;53: 4200–
547 4210. doi: 10.1128/AAC.00428-09.
- 548 36 Morvan C, Halpern D, Kénanian G, Hays C, Anba-Mondoloni J, Brinster S, et al.
549 Environmental fatty acids enable emergence of infectious *Staphylococcus aureus*

- 550 resistant to FASII-targeted antimicrobials. Nat Commun. 2016;7: 12944. doi:
551 10.1038/ncomms12944.
- 552 37 Gloux K, Guillemet M, Soler C, Morvan C, Halpern D, Pourcel C, et al. Clinical
553 Relevance of Type II Fatty Acid Synthesis Bypass in *Staphylococcus aureus*.
554 Antimicrob Agents and Chemother. 2017;61: e02515–16. doi:
555 10.1128/AAC.02515-16.
- 556 38 Kuhn S, Slavetinsky CJ, Peschel A. Synthesis and function of phospholipids in
557 *Staphylococcus aureus*. Int J Med Microbiol. 2015;305: 196-202. doi:
558 10.1016/j.ijmm.2014.12.016.
- 559 39 Lu YJ, Zhang YM, Grimes KD, Qi J, Lee RE, Rock CO. Acyl-phosphates initiate
560 membrane phospholipid synthesis in Gram-positive pathogens. Molecular Cell.
561 2006;23: 765-772. doi: 10.1016/j.molcel.2006.06.030.
- 562 40 Chaudhuri RR, Allen AG, Owen PJ, Shalom G, Stone K, Harrison M, et al.
563 Comprehensive identification of essential *Staphylococcus aureus* genes using
564 transposon-mediated differential hybridisation (TMDH). BMC Genomics.
565 2009;10: 291. doi: 10.1186/1471-2164-10-291.
- 566 41 Martin PK, Li T, Sun D, Biek DP, Schmid MB. Role in cell permeability of an
567 essential two-component system in *Staphylococcus aureus*. J Bacteriol. 1999;181:
568 3666-3673.
- 569 42 Peleg AY, Miyakis S, Ward DV, Earl AM, Rubio A, Cameron DR, et al. Whole
570 genome characterization of the mechanisms of daptomycin resistance in clinical
571 and laboratory derived isolates of *Staphylococcus aureus*. PLoS ONE. 2012;7:
572 e28316. doi: 10.1371/journal.pone.0028316.

- 573 43 Koprivnjak T, Zhang D, Ernst CM, Peschel A, Nauseef WM, Weiss JP.
574 Characterization of *Staphylococcus aureus* cardiolipin synthases 1 and 2 and their
575 contribution to accumulation of cardiolipin in stationary phase and within
576 phagocytes. J Bacteriol. 2011;193: 4134-4142. doi: 10.1128/JB.00288-11.
- 577 44 Ohniwa RL, Kitabayashi K, Morikawa K. Alternative cardiolipin synthase Cls1
578 compensates for stalled Cls2 function in *Staphylococcus aureus* under conditions
579 of acute acid stress. FEMS Microbiol Lett. 2013;338: 141-146. doi: 10.1111/1574-
580 6968.12037.
- 581 45 Peschel A, Jack RW, Otto M, Collins LV, Staubitz P, Nicholson G. *Staphylococcus*
582 *aureus* resistance to human defensins and evasion of neutrophil killing via the
583 novel virulence factor Mprf is based on modification of membrane lipids with l-
584 lysine. J Int Exp Med. 2001;193: 1067-1076. doi: 10.1084/jem.193.9.1067.
- 585 46 Nishi H, Komatsuzawa H, Fujiwara T, McCallum N, Sugai M. Reduced content of
586 lysyl-phosphatidylglycerol in the cytoplasmic membrane affects susceptibility to
587 moenomycin, as well as vancomycin, gentamicin, and antimicrobial peptides, in
588 *Staphylococcus aureus*. Antimicrob. Agents Chemother. 2004;48: 4800-4807. doi:
589 10.1128/AAC.48.12.4800-4807.2004.
- 590 47 Percy MG, Gründling A. Lipoteichoic acid synthesis and function in gram-positive
591 bacteria. Annu Rev Microbiol. 2014;68: 81-100. doi: 10.1146/annurev-micro-
592 091213-112949.
- 593 48 Fischer W. Lipoteichoic acid and lipids in the membrane of *Staphylococcus*
594 *aureus*. Med Microbiol Immunol. 1994;183: 61-76. doi: 10.1007/BF00277157.

- 595 49 Gründling A, Schneewind O. Synthesis of glycerol phosphate lipoteichoic acid in
596 *Staphylococcus aureus*. Proc Natl Acad Sci. 2007;104: 8478-8483. doi:
597 10.1073/pnas.0701821104.
- 598 50 Miller DJ, Jerga A, Rock CO, White SW. Analysis of the *Staphylococcus aureus*
599 DgkB structure reveals a common catalytic mechanism for the soluble
600 diacylglycerol kinases. Structure. 2008;16: 1036-1046. doi:
601 10.1016/j.str.2008.03.019.
- 602 51 Corrigan RM, Abbott JC, Burhenne H, Kaeffer V, Gründling A. c-di-AMP Is a New
603 Second Messenger in *Staphylococcus aureus* with a Role in Controlling Cell Size
604 and Envelope Stress. PLoS Pathog. 2011;7: e1002217. doi:
605 10.1371/journal.ppat.1002217.
- 606 52 Chaudhuri RR, Allen AG, Owen PJ, Shalom G, Stone K, Harrison M, et al.
607 Comprehensive identification of essential *Staphylococcus aureus* genes using
608 transposon-mediated differential hybridisation (TMDH). BMC Genomics.
609 2009;10: 291. doi: 10.1186/1471-2164-10-291.
- 610 53 Kobayashi K, Ehrlich SD, Albertini A, Amati G, Andersen KK, Arnaud M, et al.
611 Essential *Bacillus subtilis* genes. Proc Natl Acad Sci. 2003;100: 4678-4683. doi:
612 10.1073/pnas.0730515100.
- 613 54 Tanaka K, Henry CS, Zinner JF, Jolivet E, Cohoon MP, Xia F, et al. Building the
614 repertoire of dispensable chromosome regions in *Bacillus subtilis* entails major
615 refinement of cognate large-scale metabolic model. Nucleic Acids Research.
616 2013;41: 687-699. doi: 10.1093/nar/gks963.
- 617 55 Thanassi JA, Hartman-Neumann SL, Dougherty TJ, Dougherty BA, Pucci MJ.
618 Identification of 113 conserved essential genes using a high-throughput gene

- 619 disruption system in *Streptococcus pneumoniae*. Nucleic Acids Research.
620 2002;30: 3152-3162. doi: 10.1093/nar/gkf418.
- 621 56 Song JH, Ko KS, Lee JY, Baek JY, Oh WS, Yoon HS, et al. Identification of essential
622 genes in *Streptococcus pneumoniae* by allelic replacement mutagenesis. Mol
623 Cells. 2005;19: 365-74.
- 624 57 Behr T, Fischer W, Peter-Katalinic J, Egge H. The structure of pneumococcal
625 lipoteichoic acid. Improved preparation, chemical and mass spectrometric
626 studies. Eur J Biochem. 1992;207: 1063–1075. doi: 10.1111/j.1432-
627 1033.1992.tb17143.x.
- 628
629

630 **Supporting Information**

631 **S1 Figure. A) Daughter ion spectra in negative mode of C32:0 PG (m/z 721 [M-H]⁻) and B)**
632 **Daughter ion spectra of C32:1 PG (m/z 719 [M-H]⁻).** The insets show representative
633 structures of the lipids (with straight chain fatty acids for simplicity) detailing some of the
634 characteristic daughter ion fragments.

635

636 **S2 Figure. Daughter ion spectra in positive mode of C32:0 Glc₂-DAG (m/z 915 [M+Na]⁺).**
637 The inset shows a representative structure of the lipid (with straight chain fatty acids for
638 simplicity) detailing some of the characteristic daughter ion fragments. A common ESI-MS
639 contaminant in positive mode is highlighted by *.

640

641 **S3 Figure. Daughter ion spectra in negative mode of major C32:0 lysyl-PG species (m/z 849**
642 **[M-H]⁻).** The inset shows a representative structure of the lipid (with straight chain fatty
643 acids for simplicity) detailing some of the characteristic daughter ion fragments.

644

645 **S4 Figure. Survey scans in negative mode (1300-1450 m/z) of cardiolipin in *S. aureus***
646 **strains A) BB270 and B) Newman.** Both major [M-2H+Na]⁻ and minor [M-H]⁻ ions are
647 highlighted alongside [2(M-H)+Na]⁻ dimers of abundant PG lipids (*).

648

649 **S5 Figure. Precursor ion scans in negative mode of *S. aureus* BB270 showing**
650 **phosphatidylglycerol species as A) Parent ions of m/z 239 and B) Parent ions of m/z 267.**

651 The fatty acid compositions for the alternative mass isomers identified in the other parent
652 ion scan are written in grey.

653

654 **S6 Figure. Survey scan in negative mode (640-800 m/z) of phosphatidylglycerol species**
655 **from A) *S. aureus* Newman cultured in Tryptic Soy Broth and for comparison B) *S. aureus***
656 **Newman cultured in Müller-Hinton Broth.** Note that the survey scan shown here in panel B
657 is identical to that displayed in Figure 2 panel B.

658

659 **S1 Table. Genes with putative functions in fatty acid biosynthesis.** Specific genes (as illustrated in
660 figure 1C) are listed from the genomes of *S. aureus* strains NCTC 8325 (parent strain of BB270),
661 Newman and Mu50. Included (though not illustrated in Figure 1C) are the type II fatty acid
662 biosynthesis genes (FASII) designated 'Fab'. Homologous genes from other Gram-positive bacteria,
663 *Streptococcus pneumoniae* R6 and *Bacillus subtilis* 168, are shown for comparison. Genes in bold
664 have been designated essential based on genetic disruption in *S. aureus* NCTC8325 [52], *B. subtilis*
665 168 [53,54] and *S. pneumoniae* R6 [55].

666

667 **S2 Table: All characterised lipid species detailing composition and acyl chain position.** Based upon
668 fragmentations of lipids from all three *S. aureus* strains: BB270, Newman and Mu50.

669

670 **S3 Table. Genes with putative functions in lipid biosynthesis.** Specific genes (as illustrated
671 in Figure 5) are listed from the genomes of *S. aureus* strains NCTC 8325 (parent strain of
672 BB270), Newman and Mu50. Homologous genes from other Gram-positive bacteria,

673 *Streptococcus pneumoniae* (strain R6) and *Bacillus subtilis* (strain 168), are shown for
674 comparison. Genes in bold have been designated essential based on transposon
675 mutagenesis analysis in *S. aureus* NCTC8325 [52], *B. subtilis* 168 [53,54] and *S. pneumoniae*
676 R6 [55,56]. *Note that *S. pneumoniae* LTA has a distinct chemical composition to that of *S.*
677 *aureus* LTA [57] and thus the *LtaA* and *LtaS* genes are unrelated.

678

679

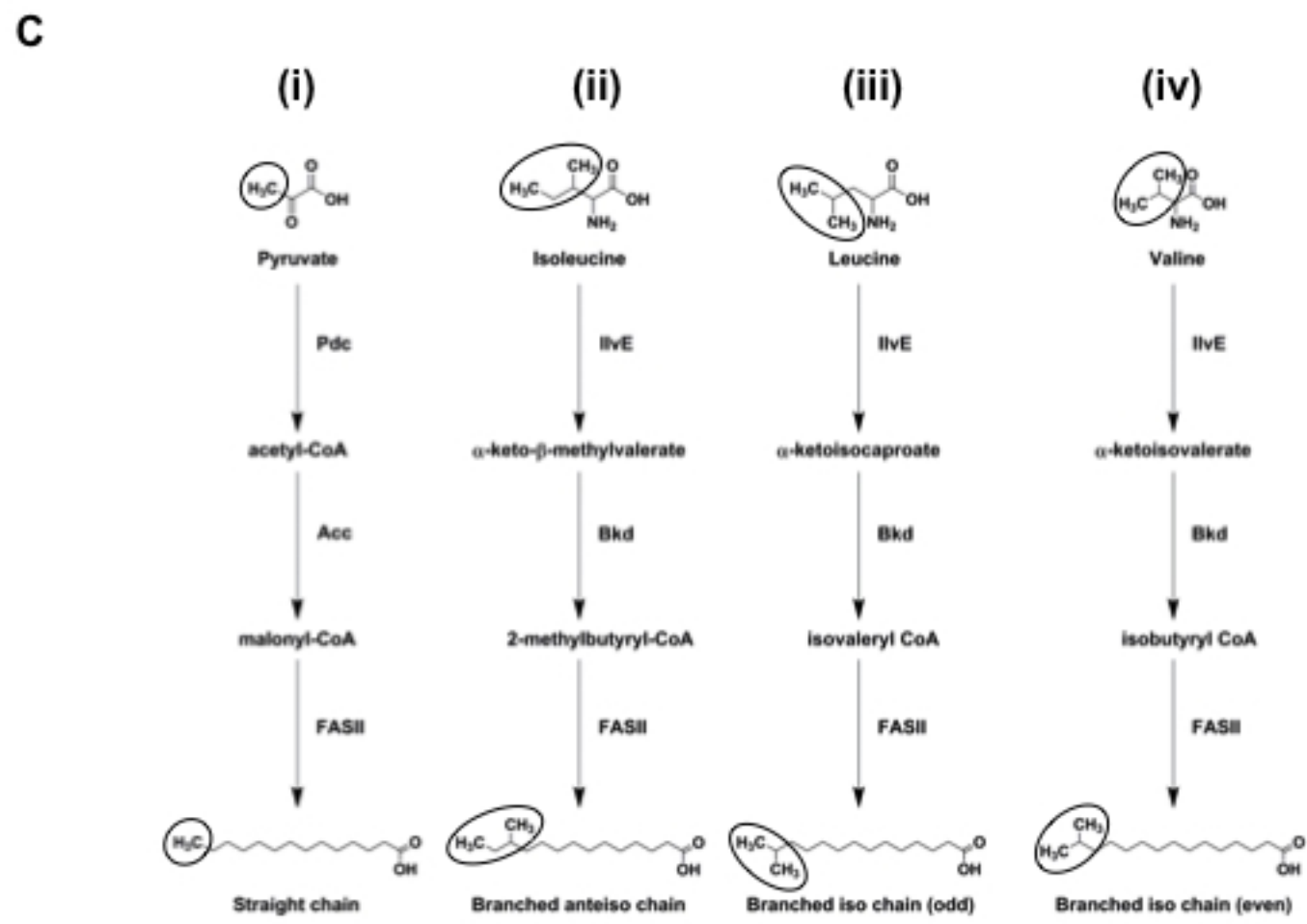
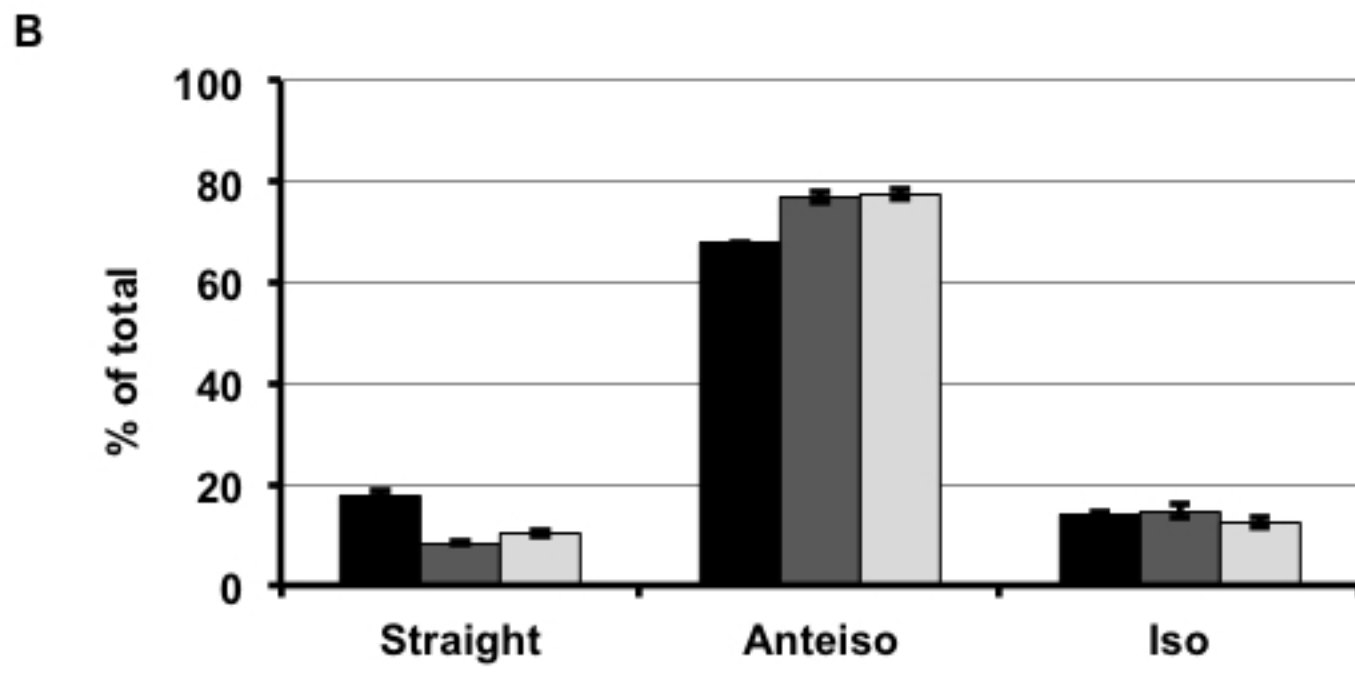
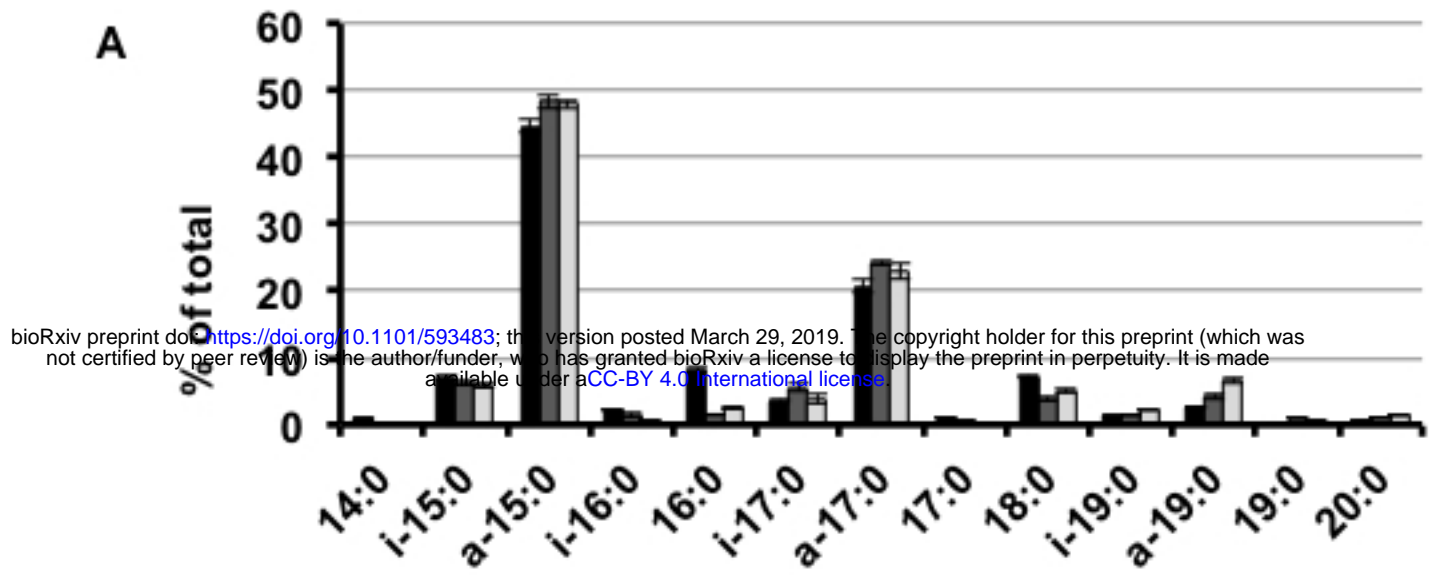


Figure 1

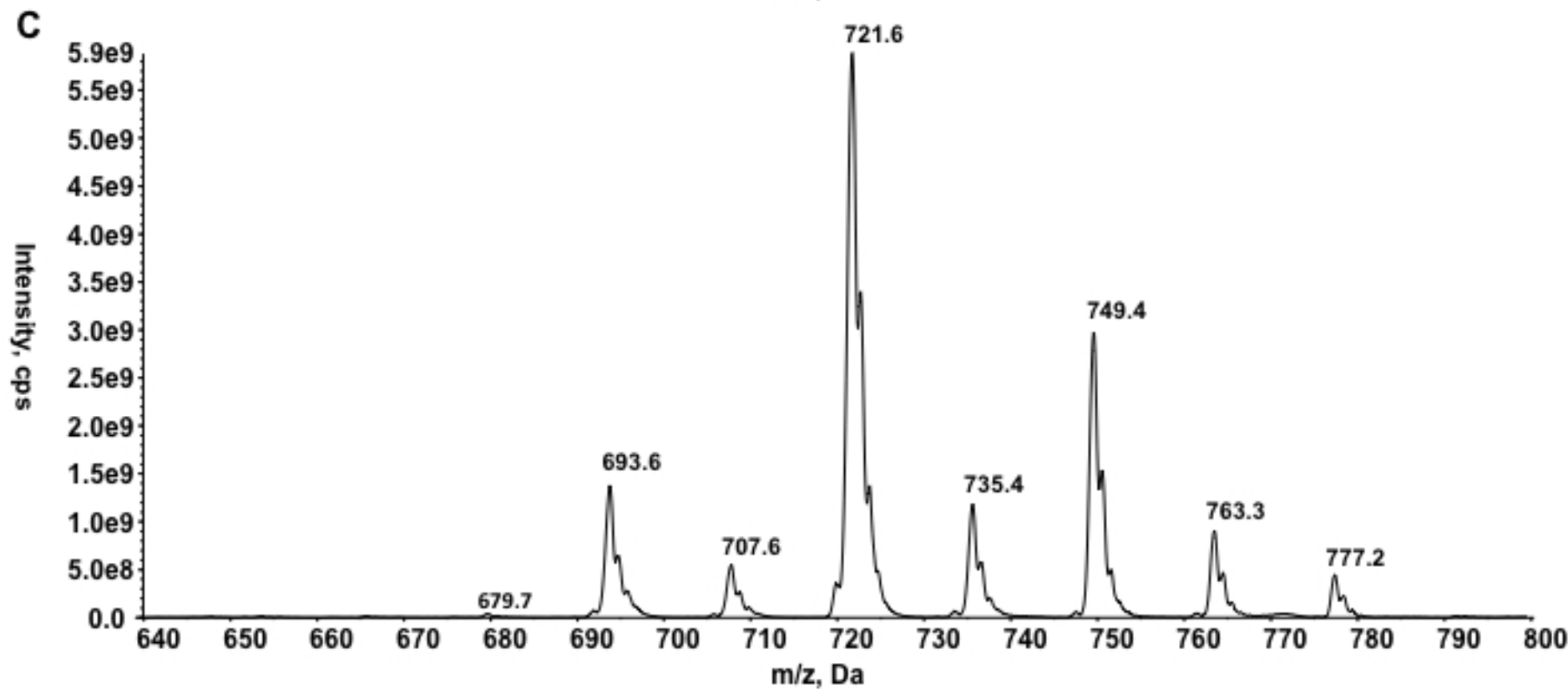
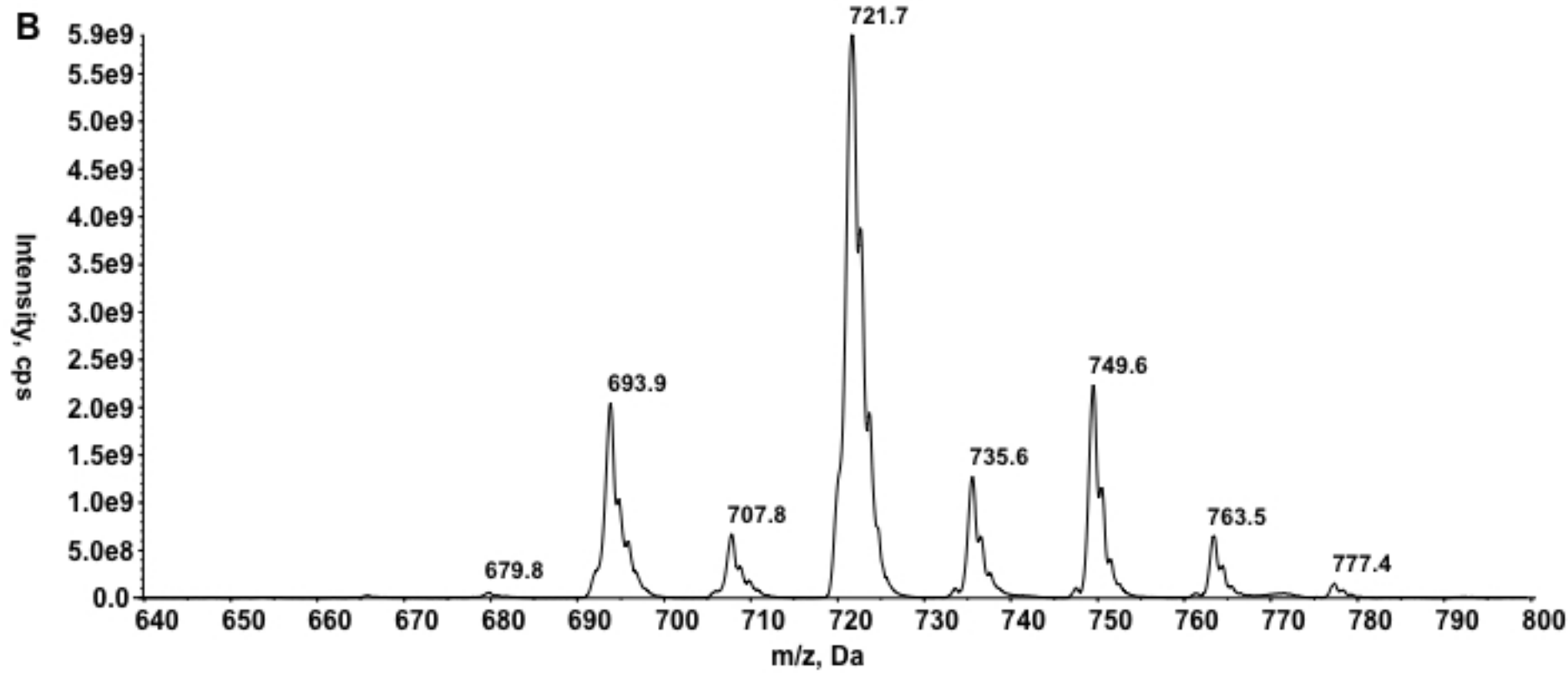
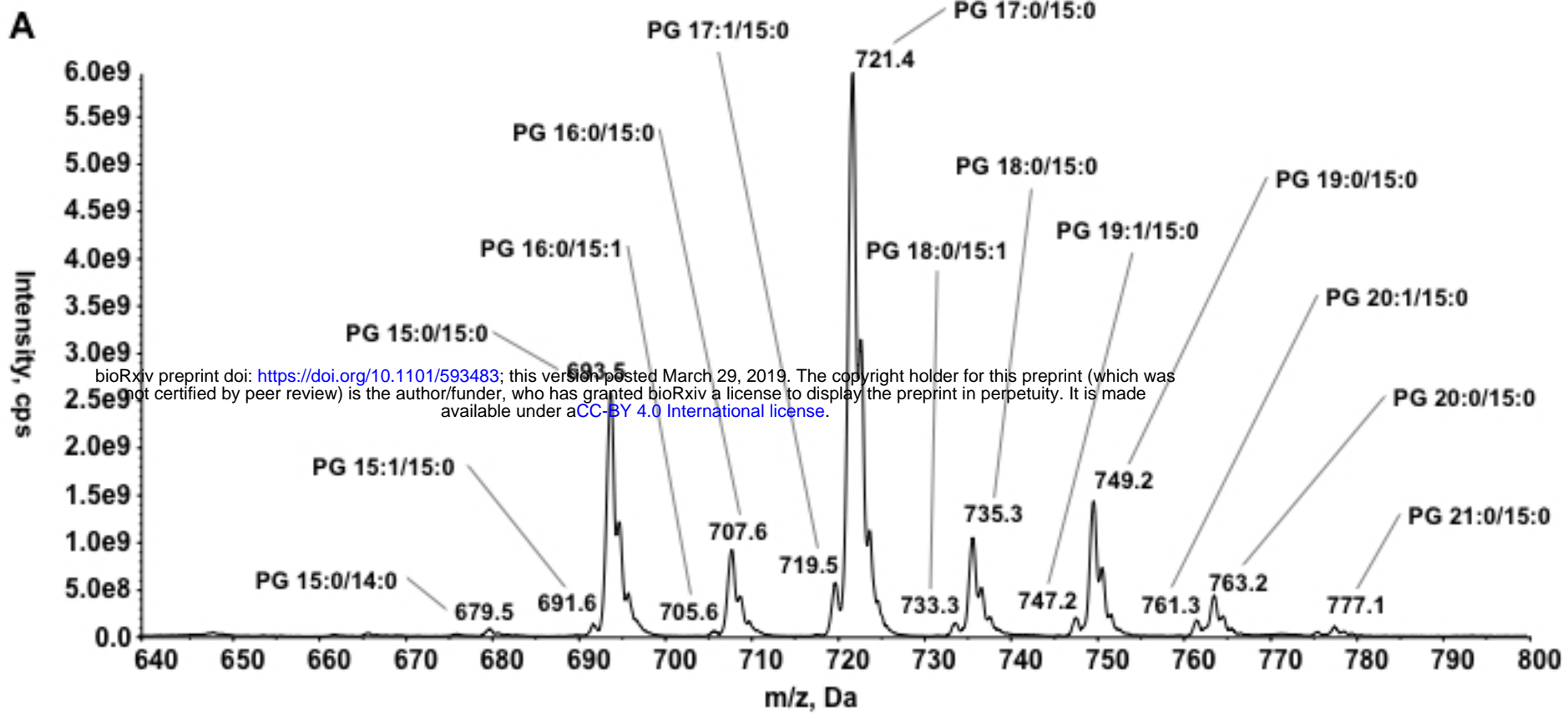


Figure 2

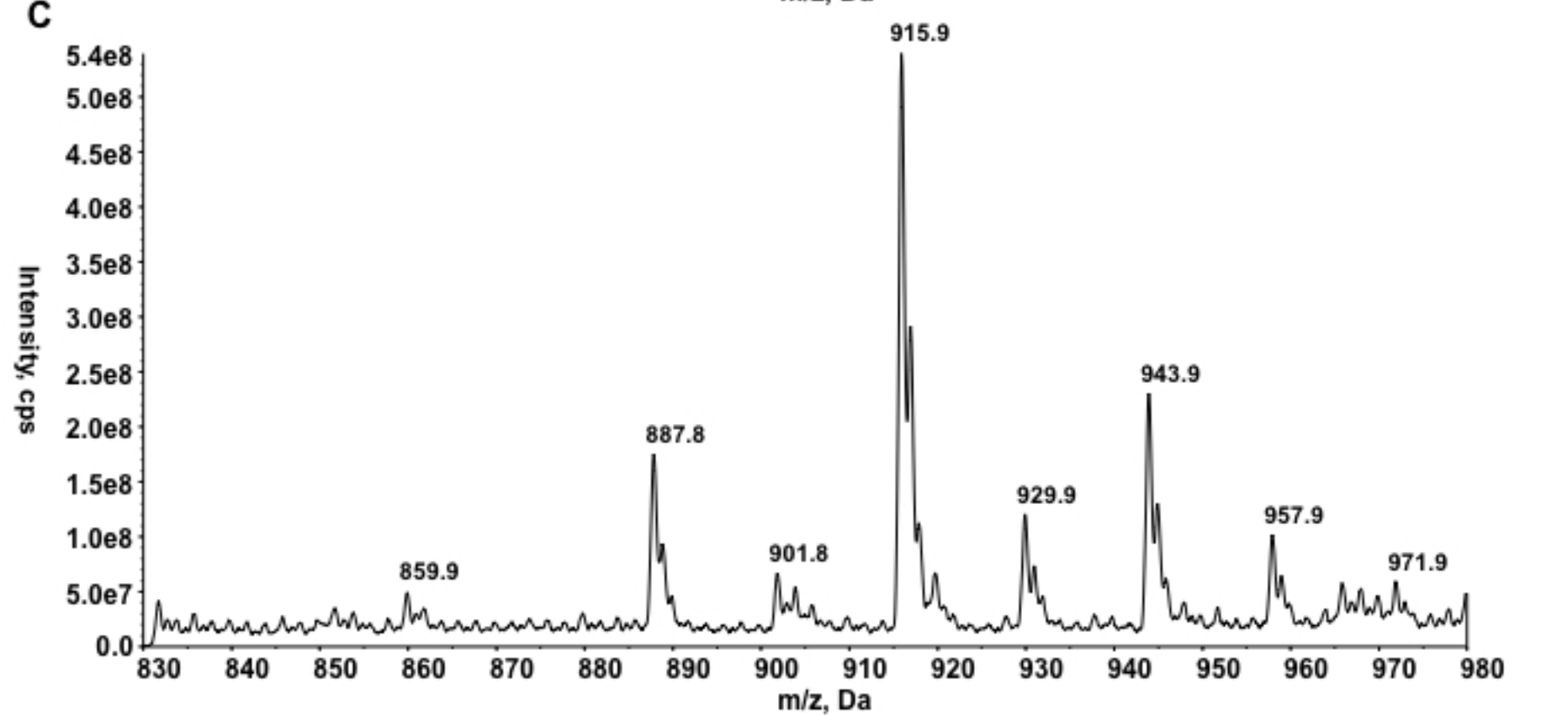
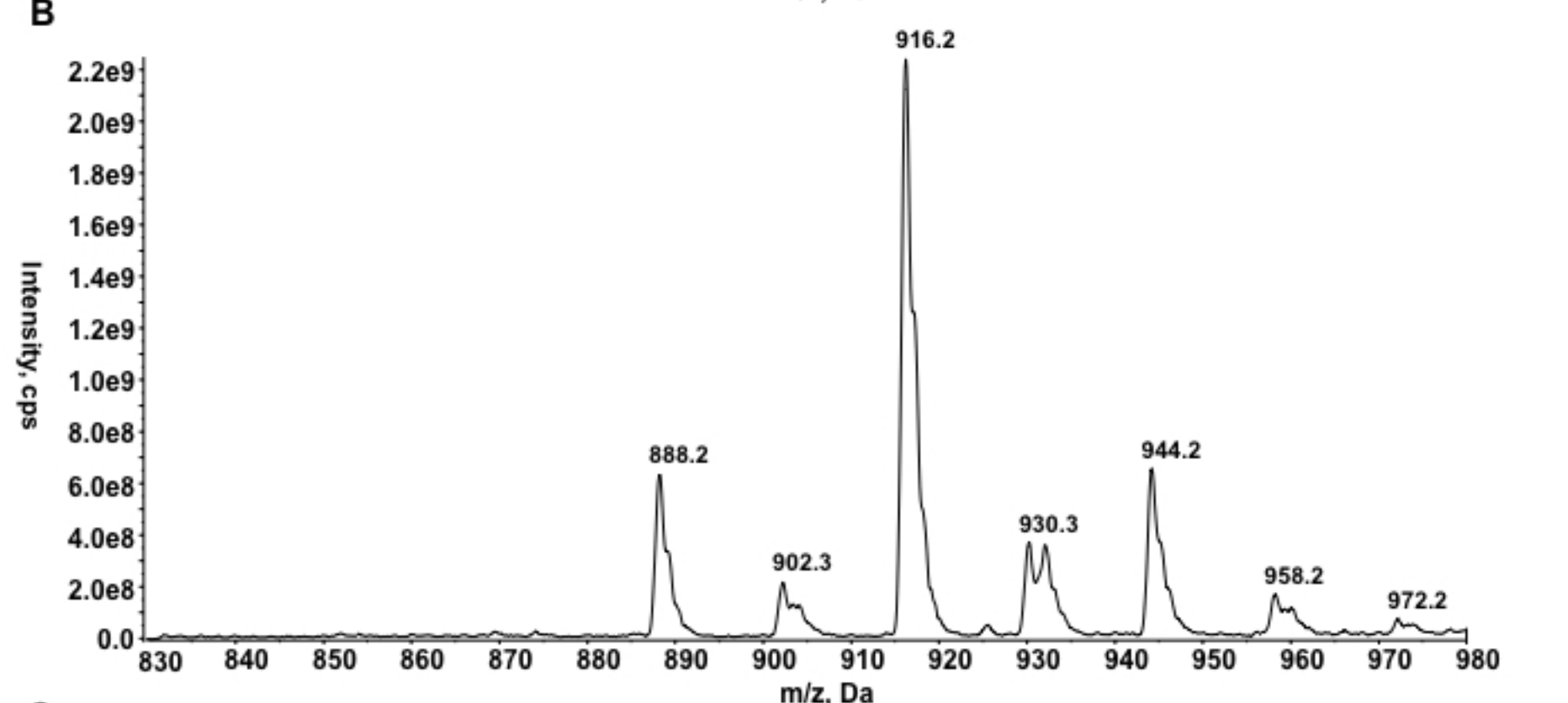
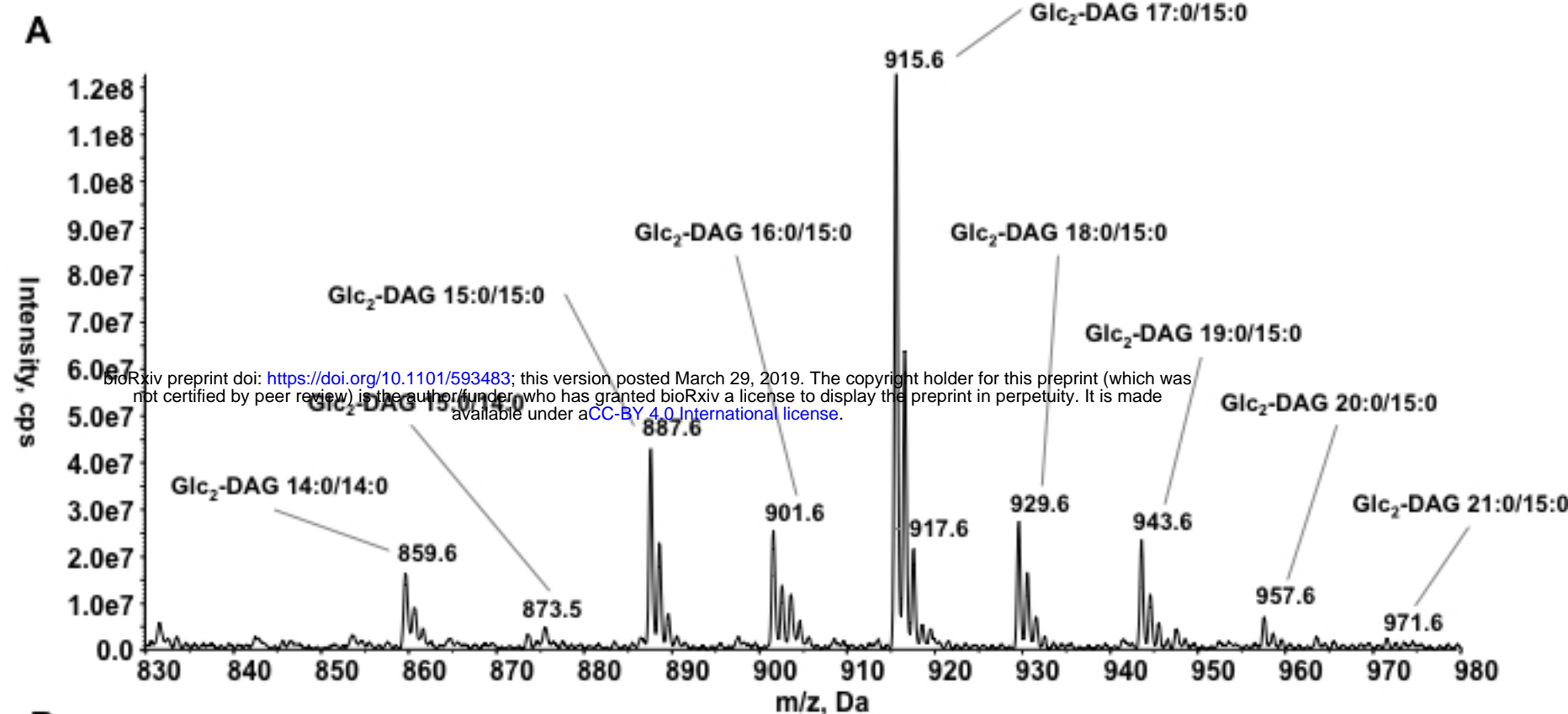


Figure 3

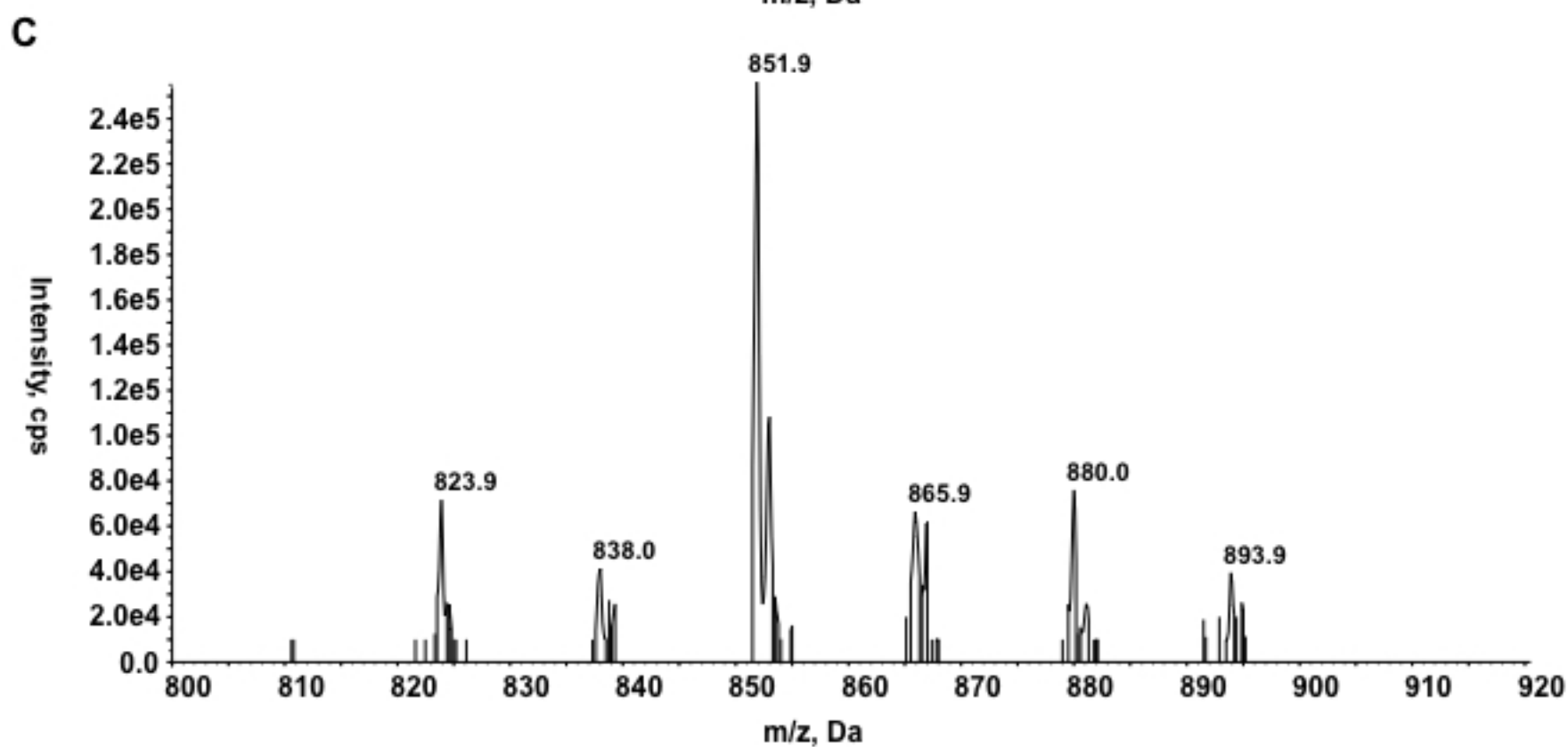
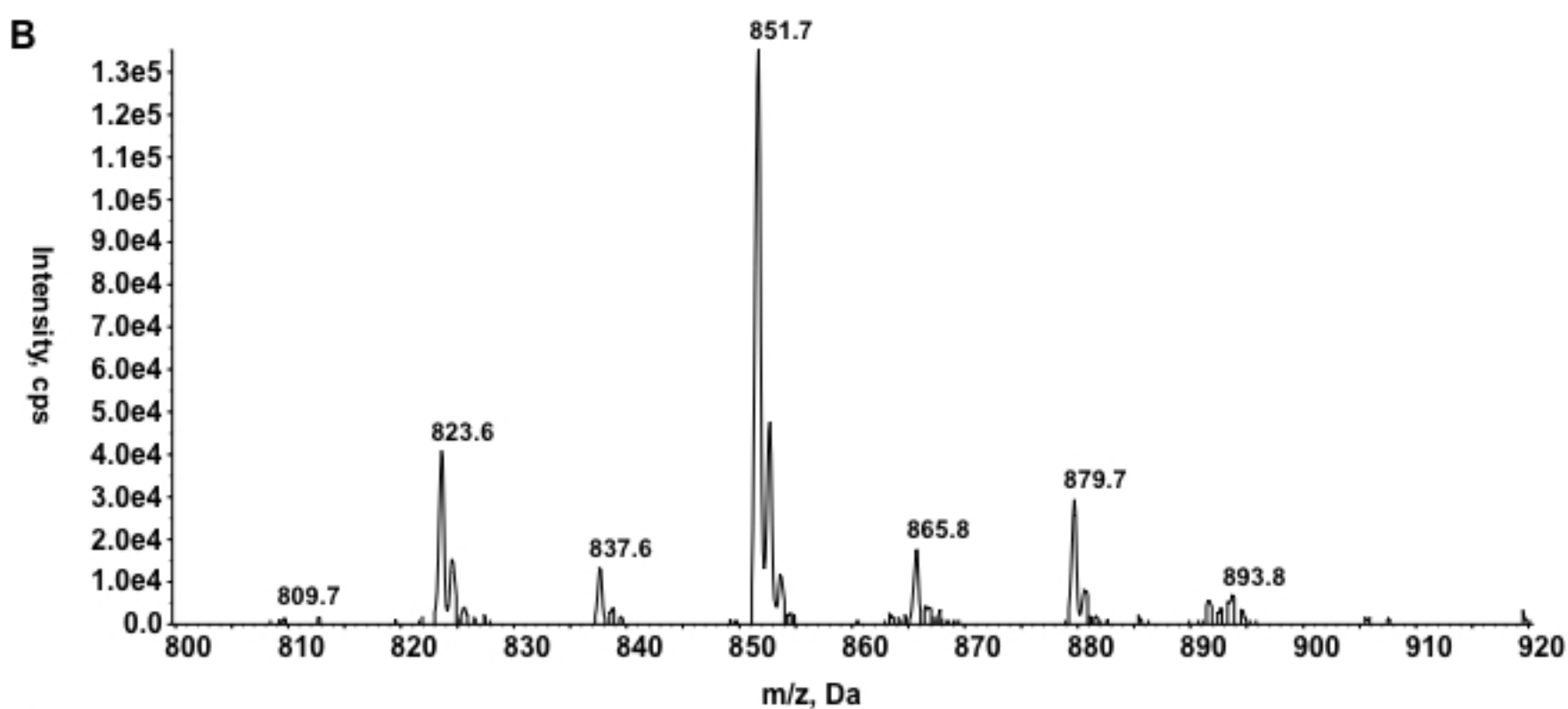
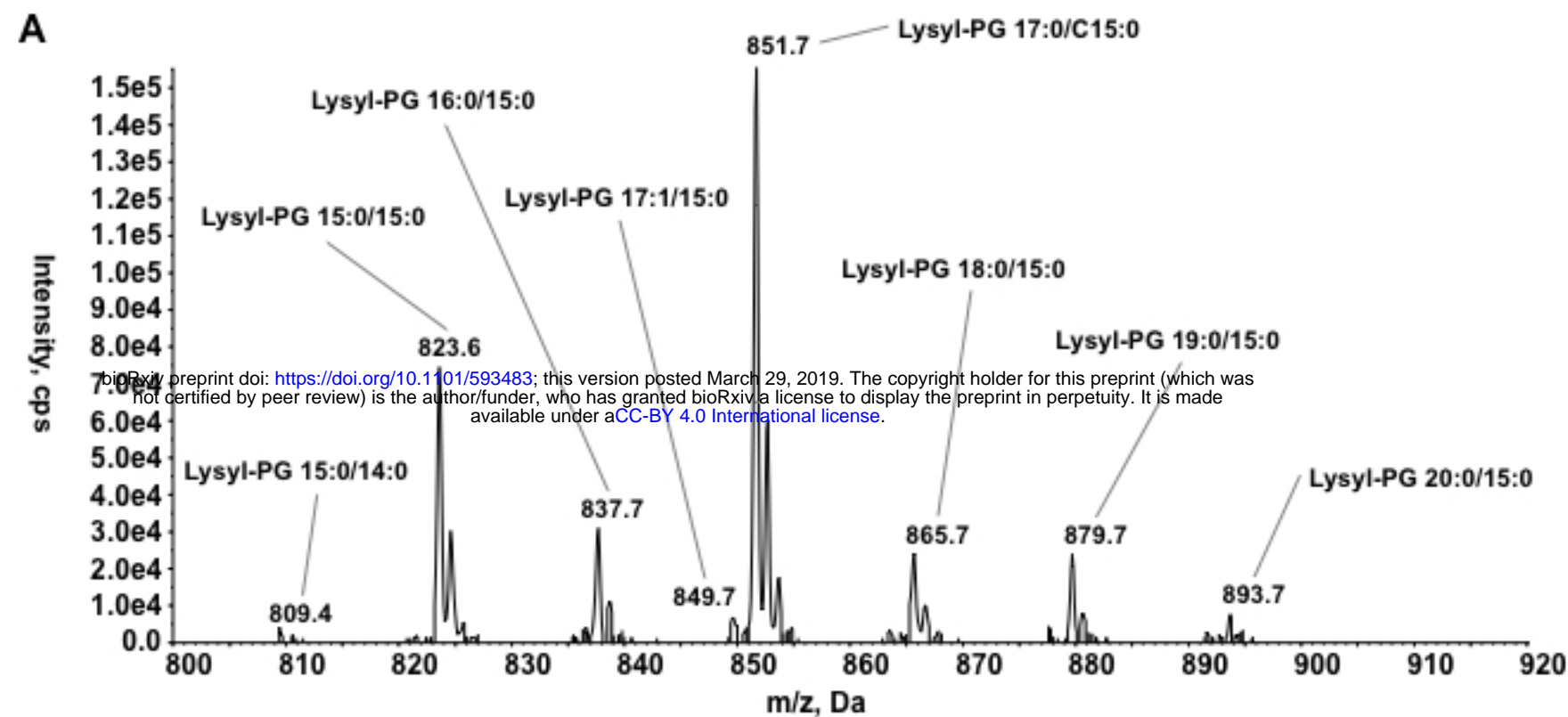


Figure 4

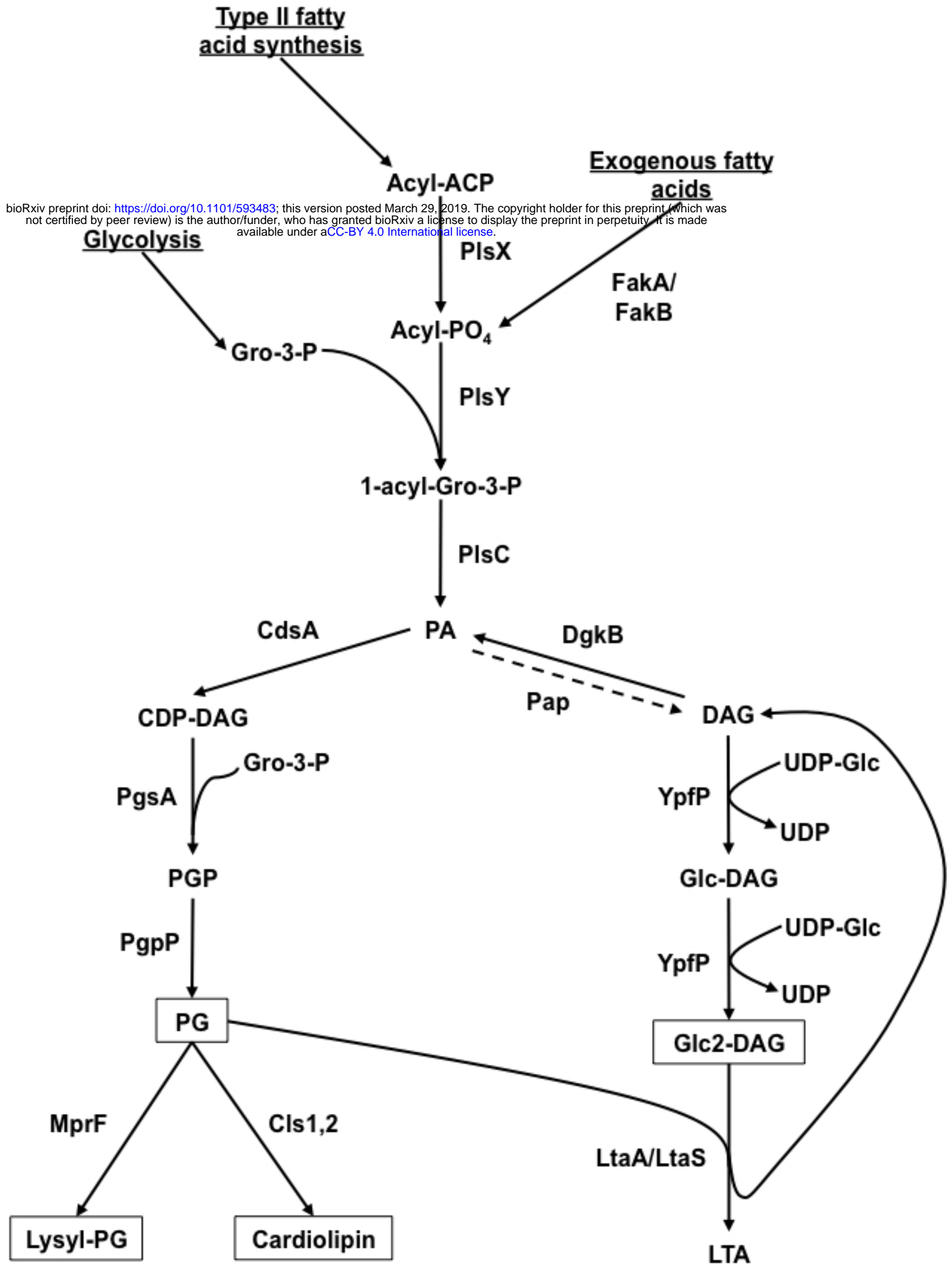


Figure 5